SPECIAL TOPIC — Silicene

Antiferromagnetic and topological states in silicene: A mean field study*

Liu Feng(刘 峰)[a)b)], Liu Cheng-Cheng(刘铖铖)[b)], and Yao Yu-Gui(姚裕贵)[b)†]

[a)] State Key Laboratory of Nonlinear Mechanics, Institute of Mechanics, Chinese Academy of Sciences, Beijing 100190, China

[b)] School of Physics, Beijing Institute of Technology, Beijing 100081, China

(Received 5 June 2015; revised manuscript received 29 June 2015; published online 20 July 2015)

It has been widely accepted that silicene is a topological insulator, and its gap closes first and then opens again with increasing electric field, which indicates a topological phase transition from the quantum spin Hall state to the band insulator state. However, due to the relatively large atomic spacing of silicene, which reduces the bandwidth, the electron–electron interaction in this system is considerably strong and cannot be ignored. The Hubbard interaction, intrinsic spin orbital coupling (SOC), and electric field are taken into consideration in our tight-binding model, with which the phase diagram of silicene is carefully investigated on the mean field level. We have found that when the magnitudes of the two mass terms produced by the Hubbard interaction and electric potential are close to each other, the intrinsic SOC flips the sign of the mass term at either K or K' for one spin and leads to the emergence of the spin-polarized quantum anomalous Hall state.

Keywords: spin-polarized quantum anomalous Hall state, silicene, antiferromagnetic state

PACS: 75.75.–c, 73.43.–f, 71.70.Ej, 73.22.–f **DOI:** 10.1088/1674-1056/24/8/087503

1. Introduction

Silicene, a monolayer honeycomb structure of silicon atoms, considered as a cousin of graphene, has aroused much concerns and is studied both theoretically and experimentally.[1–17] Because of the similar honeycomb lattice, silicene inherits most of marvellous properties in graphene including the linear energy–momentum dispersion relation and also the topological properties. On the other hand, the unique low-buckled geometry of silicene results in some outstanding properties, such as the observable quantum spin Hall effect (QSHE) in an experimentally accessible temperature[2] and the tunable electrical band gap under a perpendicular electric field,[5,6] which is considered to be a major obstacle for applications of graphene in devices. What is more, since the inversion symmetry of silicene could be broken by this electric field, some novel topological states can also be induced.[7,8,10]

When referring to the geometrical features of "honeycomb lattice" and "height differences for sublattices", silicene is not the only candidate that comes to mind, actually, bilayer graphene (BLG) does also have these features. Recently, several experiments showed clear evidences that BLG at the charge neutrality point had a gapped ground state (the magnitude of the gap is about 2 meV),[18–23] where the original degeneracy is considered to be lifted by the formation of certain ordered ground states. Since the nearly quadratic dispersion at low energy leads to finite density of states at the Fermi level, the system is susceptible to even weak interactions. Considering pseudospin (i.e., which layer), valley, and real electron spin degrees of freedom, various broken-symmetry phases have been predicted or considered.[24–39] Among these phases, the antiferromagnetic (AFM) state[31,36–39] is considered to be the most possible one, due to its consistency with the later observations including their response to a perpendicular electric field[18,23] and tilted magnetic field.[22] Noticing the striking similarity between BLG and silicene, the electron–electron interaction might induce magnetism for silicene, and the competition between the magnetic state and topological state may lead to new physics, which is worthwhile to be carefully studied.

In this paper, with the Hubbard interaction, intrinsic SOC and electric field in our tight-binding model, a systematic investigation on the phase diagram of silicene is provided. The paper is organized as follows: in Section 2, first-principle calculations of silicene are revisited. Then, the tight-binding model is introduced in Section 3 and the corresponding phase diagram is given in Section 4. We conclude this paper in Section 5 with a brief summary.

2. First-principle results

The electronic structure of silicene is obtained self-consistently by using the PAW (projector augmented

*Project supported by the National Key Basic Research Program of China (Grant Nos. 2014CB920903, 2013CB921903, 2011CBA00108, and 2012CB937500), the National Natural Science Foundation of China (Grant Nos. 11021262, 11172303, 11404022, 11225418, and 11174337), the Specialized Research Fund for the Doctoral Program of Higher Education of China (Grant No. 20121101110046), the Excellent Young Scholars Research Fund of Beijing Institute of Technology (Grant No. 2014CX04028), and the Basic Research Funds of Beijing Institute of Technology (Grant No. 20141842001).

†Corresponding author. E-mail: ygyao@bit.edu.cn

© 2015 Chinese Physical Society and IOP Publishing Ltd

wave) pseudopotential method implemented in the VASP package.[40] The exchange-correlation potential is treated by PBE (Perdew–Burke–Ernzerhof) potential.[41]

In our PBE + SOC calculations, the k-mesh is $33\times33\times1$, the energy cutoff and convergence criteria are set to be 400 eV and 10^{-6} eV respectively. The geometry and first Brillouin zone of silicene can be found in Figs. 1(a) and 1(b). The band structure of the quantum spin Hall (QSH) state is given in Fig. 1(c), and the gap is about 1.5 meV.[2,5]

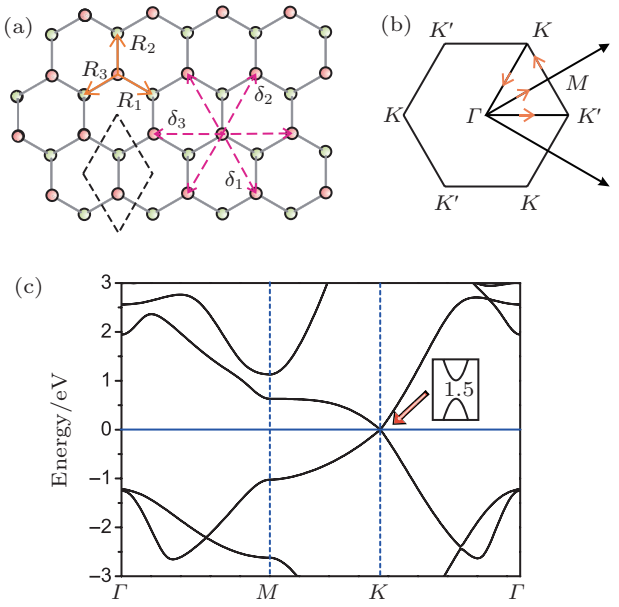


Fig. 1. Geometry, Brillouin zone, and electronic structure. (a) The geometry of silicene. (b) The corresponding Brillouin zone. (c) The band structure of the QSH state, where the inset is the zooming gap with size marked, and the unit is in meV.

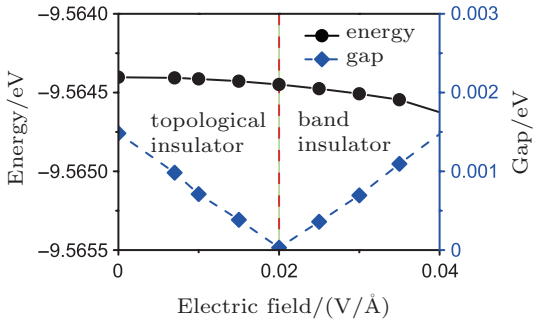


Fig. 2. The energy and band gap with respect to the perpendicular electric field through first-principle calculations. The critical electric field 0.02 V/Å is marked with red dash line, which separates the topological insulator state from the band insulator state (topological trivial).

The low-buckled geometry, which makes silicene different from graphene, can be well taken advantage of by applying an electric field. Therefore, we investigated the behavior of the band gap and energy with respect to the perpendicular electric field. In Fig. 2, one can see with an increasing electric field the band gap of the QSH state first closes then opens again, which is the consequence of topological phase transition,[9] and the critical electric field (about 0.02 V/Å) is consistent with Ref. [5]. The first principle calculations help us understand the basic electrical properties of silicene based on single electron approximation. However, due to the relatively large atomic spacing of silicene, which reduces the bandwidth, the electron–electron interaction in this system is considerably strong and cannot be ignored,[42] and therefore a further investigation on the influence of electron–electron interaction to silicene is needed.

3. Tight-binding model

The Hubbard interaction, SOC, and electric field are taken into consideration in our tight-binding model, and the total Hamiltonian is given as $H = H_0 + H_U + H_V$. The first term H_0 is the low-energy effective Hamiltonian involving the SOC in silicene introduced in Ref. [3]:

$$H_0 = -t\sum_{\langle ij\rangle\alpha} c^{\dagger}_{i\alpha}c_{j\alpha} + \mathrm{i}\frac{\lambda_{\mathrm{SO}}}{3\sqrt{3}}\sum_{\langle\langle ij\rangle\rangle\alpha\beta} \nu_{ij}c^{\dagger}_{i\alpha}\boldsymbol{\sigma}^{z}_{\alpha\beta}c_{j\beta} - \mathrm{i}\frac{2}{3}\lambda_{R_2}\sum_{\langle\langle ij\rangle\rangle\alpha\beta}\mu_{ij}c^{\dagger}_{i\alpha}(\boldsymbol{\sigma}\times\hat{d}_{ij})^{z}_{\alpha\beta}c_{j\beta}, \quad (1)$$

where $c^{\dagger}_{i\alpha}$ is a creation operator for an electron with spin α on site i. The first term in Eq. (1) represents the usual nearest neighbor hopping term. The second term in Eq. (1) is the intrinsic SOC, where $\nu_{ij} = (\boldsymbol{d}_i\times\boldsymbol{d}_j)/|\boldsymbol{d}_i\times\boldsymbol{d}_j|$, and $\boldsymbol{d}_i$ and $\boldsymbol{d}_j$ are two nearest bonds connecting the next-nearest neighbor sites. The third term in Eq. (1) is the intrinsic Rashba SOC, and $\hat{d}_{ij} = d_{ij}/|d_{ij}|$, where d_{ij} represents a vector from site j to i and $\mu_{ij} = \pm1$ for A or B site. The summation over $\langle ij\rangle$ ($\langle\langle ij\rangle\rangle$) runs over all the nearest (next-nearest) neighbor sites. Note that the values of the above coupling parameters are given by Ref. [3], that is $t = 1.12$ eV, $\lambda_{\mathrm{SO}} = 3.9$ meV, and $\lambda_{R_2} = 0.7$ meV. Since the relatively small value of λ_{R_2} and also to facilitate following derivations and discussions, we let $\lambda_{R_2} = 0$ meV.

The second term H_U is the Hubbard interaction, to be exact,

$$H_U = U\sum_i n_{i\uparrow}n_{i\downarrow}, \quad (2)$$

and U represents the Hubbard interaction strength. The fluctuation term $U\sum_i(n_{i\uparrow}-\langle n_{i\uparrow}\rangle)(n_{i\downarrow}-\langle n_{i\downarrow}\rangle)$ is omitted under the mean field approximation. To discuss the electric field effect in silicene, we add the third term, i.e., the staggered potential term

$$H_V = -\sum_{i\alpha}\frac{(-1)^l V}{2}c^{\dagger}_{i\alpha}c_{i\alpha}, \quad (3)$$

where $l = 1, 0$ correspond to A and B sublattices respectively. The total Hamiltonian can be transformed into a 4×4 matrix $H(\boldsymbol{k})$ for each crystal momentum $\boldsymbol{k}$ on the basis of $\{\psi_{A\uparrow}, \psi_{B\uparrow}, \psi_{A\downarrow}, \psi_{B\downarrow}\}$

$$H(\boldsymbol{k}) = H_0(\boldsymbol{k}) + H_U(\boldsymbol{k}) + H_V(\boldsymbol{k}), \quad (4)$$

and $H_0(\boldsymbol{k})$, $H_U(\boldsymbol{k})$, and $H_V(\boldsymbol{k})$ are given as follows:

$$H_0(\boldsymbol{k}) = \begin{pmatrix} h(\boldsymbol{k}) & -tf(\boldsymbol{k}) & 0 & 0 \\ -tf(\boldsymbol{k})^* & -h(\boldsymbol{k}) & 0 & 0 \\ 0 & 0 & -h(\boldsymbol{k}) & -tf(\boldsymbol{k}) \\ 0 & 0 & -tf(\boldsymbol{k})^* & h(\boldsymbol{k}) \end{pmatrix}, \quad (5)$$

$$H_U(\boldsymbol{k}) = \begin{pmatrix} U\langle n_{a\downarrow}\rangle & 0 & 0 & 0 \\ 0 & U\langle n_{b\downarrow}\rangle & 0 & 0 \\ 0 & 0 & U\langle n_{a\uparrow}\rangle & 0 \\ 0 & 0 & 0 & U\langle n_{b\uparrow}\rangle \end{pmatrix}, \quad (6)$$

$$H_V(\boldsymbol{k}) = \begin{pmatrix} V/2 & 0 & 0 & 0 \\ 0 & -V/2 & 0 & 0 \\ 0 & 0 & V/2 & 0 \\ 0 & 0 & 0 & -V/2 \end{pmatrix}, \quad (7)$$

where $f(\boldsymbol{k}) = \sum_\alpha \mathrm{e}^{\mathrm{i}\boldsymbol{k}\cdot\boldsymbol{R}_\alpha}$, with $\boldsymbol{R}_\alpha$ ($\alpha = 1,2,3$) to be the nearest-neighbor vector, and $h(\boldsymbol{k}) = -(2/3\sqrt{3})\lambda_{\mathrm{SO}}\sum_\alpha \sin(\boldsymbol{k}\cdot\boldsymbol{\delta}_\alpha)$, with $\boldsymbol{\delta}_\alpha$ ($\alpha = 1,2,3$) to be the next nearest-neighbor vector, which is shown in Fig. 1(a). Now the Hubbard interaction, intrinsic SOC, and electric field are considered in our tight-binding model, and each ingredient is essential to the following discussion.

3.1. The case without SOC

In the case without SOC, using the Hamiltonian at the mean-field level given by Eqs. (4)–(7), we can solve this problem self-consistently. Note that there are two atoms in a unit cell, as shown in Fig. 1(a), and thus four mean fields are needed in our model considering spin degree of freedom. With $\lambda_{\mathrm{SO}} = 0$ and $V = 0$, the critical value $U_{\mathrm{c}} = 2.485$ eV is obtained in our calculation (see Fig. 3(a)), and $(U_{\mathrm{c}}/t) \approx 2.2$ is consistent with previous works.[43,44] With $\lambda_{\mathrm{SO}} = 0$, $V \neq 0$, and fixed $U = 2.492$ eV slightly larger than U_{c}, the variations of the gaps for different spins with respect to V are plotted in Fig. 3(b), where a first order phase transition (from the AFM state to the charge density wave (CDW) state, since the corresponding on site spin polarization $n_{i\uparrow} - n_{i\downarrow}$ vanishes during this process and the charge polarization $n_a - n_b \neq 0$) can be seen.

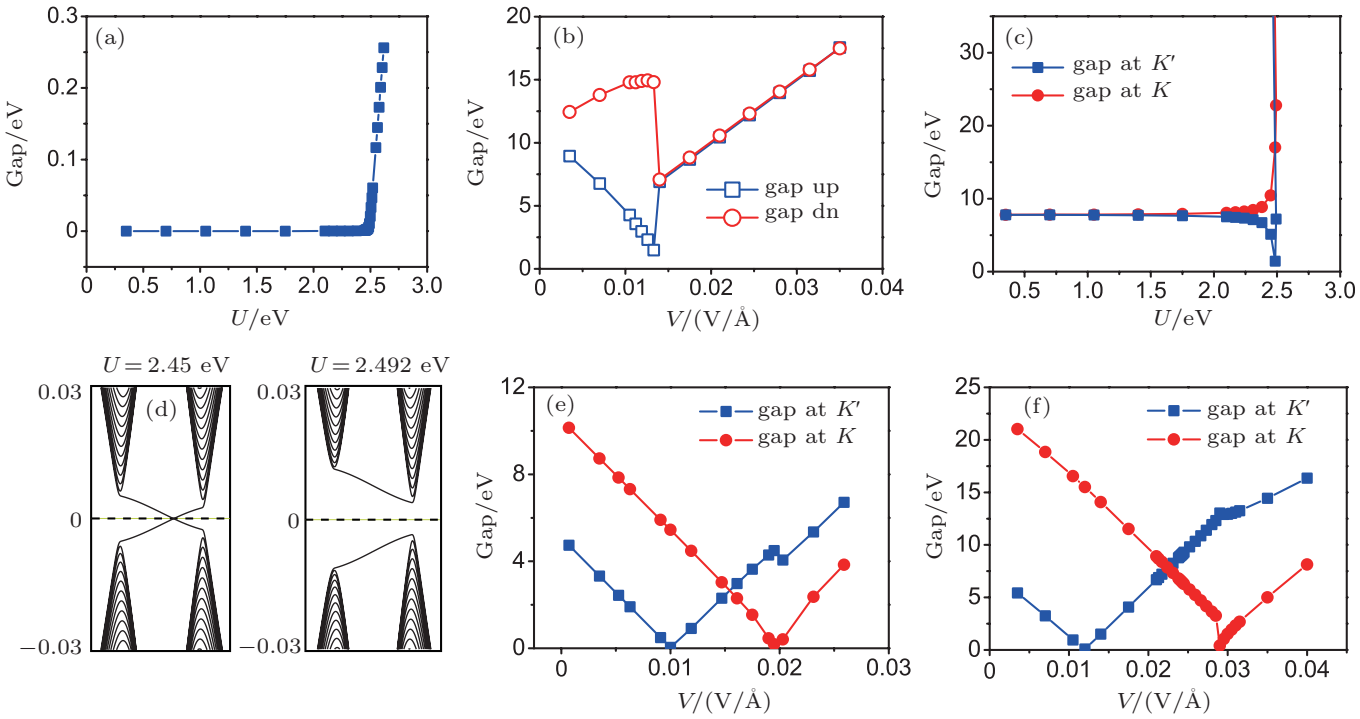


Fig. 3. The results of mean-field self-consistent calculations. (a) Without the intrinsic SOC and electric field, the band gaps at K and K' as functions of the Hubbard U. (b) Without the intrinsic SOC, the band gaps for different spins as functions of the electric potential for $U = 2.492$ eV. (c) With the intrinsic SOC and zero electric field, the band gaps at K and K' as functions of the Hubbard U, and the edge states for $U = 2.45$ eV and $U = 2.492$ eV in panel (d). With the intrinsic SOC, the band gaps at K and K' with respect to the electric potential are given in panels (e) and (f) for $U = 2.45$ eV and $U = 2.492$ eV respectively.

3.2. The case with SOC

In the case with SOC, the QSHE has been proposed in silicene,[2] by exploiting adiabatic continuity and the direct calculation of the Z_2 topological invariant. The band gap opened by the SOC is about 1.5 meV, leading to the observable QSHE in an experimentally accessible temperature. However, considering the weakness of the SOC in silicene, it would be interesting to find if there are any new phases obtained from the competition between the SOC and Hubbard interaction. Therefore their phase diagram should be systematically studied.

Here we will use the tight-binding model introduced above, with the intrinsic SOC ($\lambda_{\mathrm{SO}} = 3.9$ meV) turned on, to discuss this issue. The behavior of the gap with respect to U (see Fig. 3(c)) is nearly the same as the one without the intrinsic SOC discussed above (see Fig. 3(a)). However, the sizes

of the band gaps at K and K' become different now. For the former, with the increasing Hubbard U the gap grows slowly until the critical value about 2.485 eV, after which there will be a rapid increase. Whereas the latter changes in a different way, first the gap becomes small, but once the Hubbard U exceeds the threshold value approximately 2.485 eV, the gap turns to increase.

One is naturally invited to the question: what happened in this process, especially, whether the gap at K' closed at the vicinity of $U = 2.485$ eV, since the numerical calculation is not easy to capture this detail considering the sensitivity for parameters near the phase transition. To answer this question, we study the edge states of the zigzag edged nanoribbon of silicene. The edge states for $U = 2.45$ eV and $U = 2.492$ eV are given in Fig. 3(d), and it is obvious that there is a topological phase transition underlying this process. Therefore, the behavior of band gap is not hard to understand: when $U = 0$ eV, with the intrinsic SOC silicene is in the QSH state,[2,3] and the sign of the mass term flips at either K or K'. However, keep increasing the Hubbard U, which provides a k-spatial uniform mass term from the point view of the mean-field approximation, will finally drive the system into the topological trivial state, and at the topological phase transition point the band gap of silicene must close. We also calculate Chern number and spin-Chern number as an argument, the definition of which are $C = C_\uparrow + C_\downarrow$ and $C_s = (C_\uparrow - C_\downarrow)/2$ respectively. The results are just as we expect, for $U = 2.45$ eV $(C, C_s) = (0, -1)$ and for $U = 2.492$ eV $(C, C_s) = (0, 0)$.

We now proceed to discuss the effect of electric field to silicene. Two typical values of Hubbard $U = 2.45$ eV and $U = 2.492$ eV are chosen to study the variation of the system with respect to the electric potential V, and the entire phase diagram will be left for the next section.

With respect to the electric potential, the band gaps at K and K' are given in Figs. 3(e) and 3(f) for $U = 2.45$ eV and $U = 2.492$ eV respectively, from which we can see the gaps at K and K' both first become small, and when the electric field exceeding certain values, they start to increase. To comprehend these two processes, we investigated the evolution of the edge states with respect to the electric field shown in Figs. 4(a) and 4(b). Note that due to the first order phase transition in Fig. 4(b), we fail to capture the moment of the closure of the gap at K for $U = 2.492$ eV, but with the analysis of the edge states and also the following calculation of Chern number, this closure can be confirmed. With $U = 2.45$ eV, $(C, C_s) = (0, 1)$ (QSH) for $V = 0, 0.0035$ eV, $(C, C_s) = (1, 1/2)$ for $V = 0.0147$ eV, $(C, C_s) = (0, 0)$ (trivial) for $V = 0.0231$ eV, and the system is at the phase transition critical point when $V = 0.01, 0.0195$ eV. It is worth noting that $(C, C_s) = (1, 1/2)$ represents the system is spin-polarized, and this state is therefore named spin-polarized quantum anomalous Hall (SQAH) state.[10] For $U = 2.492$ eV, the (C, C_s) is $(0, 0)$ for $V = 0.0, 0.007, 0.029, 0.035$ eV, $(1, -1/2)$ for $V = 0.021$ eV, $V = 0.012$ eV is the phase transition critical point, and the phase transition critical point near $V = 0.029$ is not captured due to the first-order phase transition mentioned above. These two parameter paths are marked in Fig. 4(d).

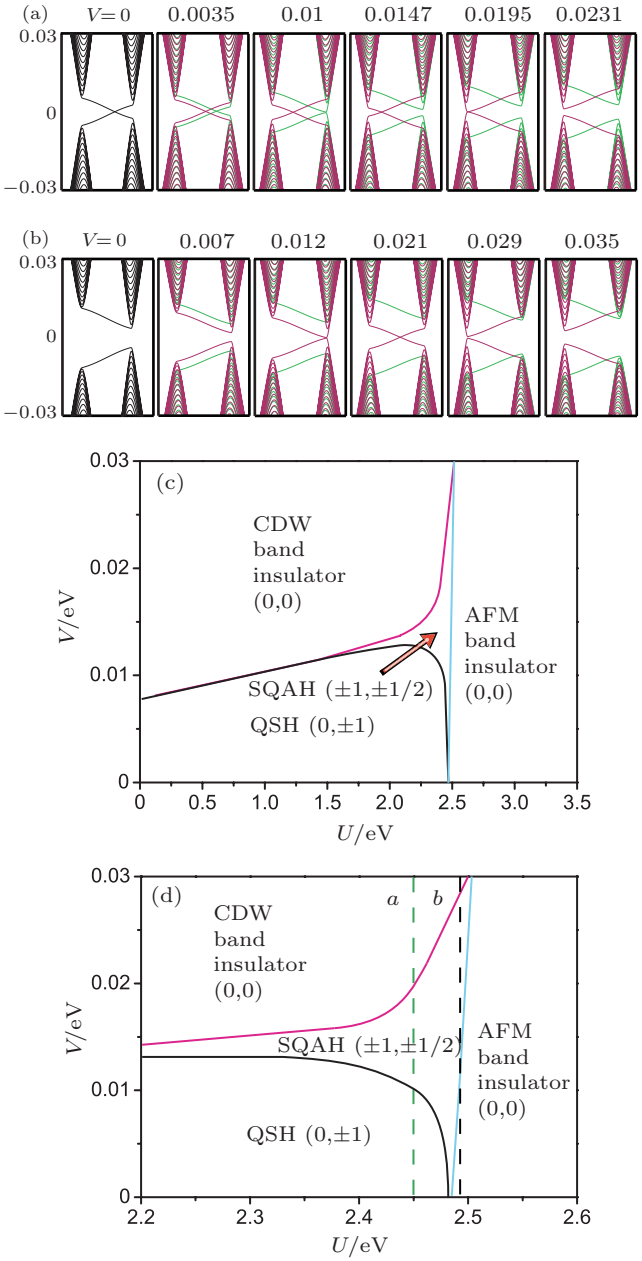


Fig. 4. (a) The edge states for $U = 2.45$ eV, with $V = 0.0$, 0.0035, 0.01, 0.0147, 0.0195, 0.0231 eV. (b) The edge states for $U = 2.492$ eV, with $V = 0.0$, 0.007, 0.012, 0.021, 0.029, 0.035 eV. Different colors represent different spins. (c) The schematic phase diagram. There are four phases as indicated by QSH state, CDW band insulator, AFM band insulator, and SQAH state. The corresponding (C, C_s) of four phases are given to help understanding. The paths of panels a and b are marked in the zooming phase diagram (d).

The physics in the above process can be understood from the competition between two different mass terms produced by the Hubbard U and electric potential V. However, due to the k-spatial uniform property of these two mass terms, the nontrivial topological state cannot be induced by themselves, and only when the magnitudes of these two mass terms are close to each other, can the intrinsic SOC flip the sign of the mass

term at either K or K' for one spin and lead to the emergence of the topological state, i.e., the SQAH state.

4. Phase diagram in (U,V) plane

After acquainting with the phase transition at a fixed Hubbard U as a function of the electric potential V, we next investigate the phase diagram for the whole (U,V) plane. Actually, all of these phases, which can be obtained in this plane, have been discussed above, and we can determine phase boundaries by scanning the points with zero band gap at K or K'.

In Fig. 4(c), there are four phases, named QSH state, CDW band insulator, AFM band insulator, and SQAH state. The results can be understood as the following aspects. When both U and V are small, the intrinsic SOC dominates, and because the gap keeps open during this adiabatic process, it must be in the same topological state as the original one, viz QSH state. To increase no matter U or V will finally drive this system turning into a trivial insulator state, for the former it will be the AFM band insulator (two sublattices have opposite spin polarization directions), while, for the later it will be the CDW band insulator (different charge densities for two sublattices). The intrinsic SOC will help to induce the SQAH state in the region where the magnitudes of the two mass terms produced by U and V are close to each other.

5. Conclusion

To summarize, the topological properties of silicene are revisited and confirmed with first principles calculations. To consider the influence of electron–electron interaction on silicene, the intrinsic SOC, Hubbard interaction, and electric field are taken into consideration in our tight-binding model on the mean-field level. Then, with this tight-binding model, the phase diagram of silicene is revealed, and we find that the appearance of the spin-polarized quantum anomalous Hall (SQAH) state stems from the competition between the electric field and Hubbard interaction.

References

[1] Guzmán-Verri G G and Lew Yan Voon L C 2007 *Phys. Rev. B* **76** 075131
[2] Liu C C, Feng W and Yao Y 2011 *Phys. Rev. Lett.* **107** 076802
[3] Liu C C, Jiang H and Yao Y 2011 *Phys. Rev. B* **84** 195430
[4] Cahangirov S, Topsakal M, Aktürk E, Sahin H and Ciraci S 2009 *Phys. Rev. Lett.* **102** 236804
[5] Drummond N D, Zólyomi V and Falḱo V I 2012 *Phys. Rev. B* **85** 075423
[6] Ni Z, Liu Q, Tang K, Zheng J, Zhou J, Qin R, Gao Z, Yu D and Lu J 2012 *Nano Lett.* **12** 113
[7] Pan H, Li Z, Liu C C, Zhu G, Qiao Z and Yao Y 2014 *Phys. Rev. Lett.* **112** 106802
[8] Ezawa M 2012 *Phys. Rev. Lett.* **109** 055502
[9] Ezawa M 2012 *New J. Phys.* **14** 033003
[10] Ezawa M 2013 *Phys. Rev. B* **87** 155415
[11] Tahir M and Schwingenschlögl U 2012 arXiv: 1207.4745v1 [cond-mat.mes-hall]
[12] Lalmi B, Oughaddou H, Enriquez H, Kara A, Vizzini S, Ealet B and Aufray B 2012 *Appl. Phys. Lett.* **97** 223109
[13] Chen L, Liu C C, Feng B, He X, Cheng P, Ding Z, Meng S, Yao Y and Wu K 2012 *Phys. Rev. Lett.* **109** 056804
[14] Feng B, Ding Z, Meng S, Yao Y, He X, Cheng P, Chen L and Wu K 2012 *Nano Lett.* **12** 3507
[15] Vogt P, De Padova P, Quaresima C, Avila J, Frantzeskakis E, Asensio M C, Resta A, Ealet B and Le Lay G 2012 *Phys. Rev. Lett.* **108** 155501
[16] Fleurence A, Friedlein R, Ozaki T, Kawai H, Wang Y and Yamada-Takamura Y 2012 *Phys. Rev. Lett.* **108** 245501
[17] Kara A, Enriquez H, Seitsonen A P, Voon L L Y, Vizzini S, Aufray B and Oughaddou H 2012 *Surface Science Reports* **67** 1
[18] Velasco J Jr, Jing L, Bao W, Lee Y, Kratz P, Aji V, Bockrath M, Lau C N, Varma C, Stillwell R, Smirnov D, Zhang F, Jung J and MacDonald A H 2012 *Nat. Nanotech.* **7** 156
[19] Freitag F, Weiss M, Maurand R, Trbovic J and Schönenberger C 2013 *Phys. Rev. B* **87** 161402
[20] Weitz R T, Allen M T, Feldman B E, Martin J and Yacoby A 2010 *Science* **330** 812
[21] Freitag F, Trbociv J, Weiss M and Schnenberger C 2012 *Phys. Rev. Lett.* **108** 076602
[22] Veligura A, van Elferen H J, Tombros N, Maan J C, Zeitler U and van Wees B J 2012 *Phys. Rev. B* **85** 155412
[23] Bao W, Velasco J Jr, Jing L, Zhang F, Standley B, Smirnov D, Bockrath M, MacDonald A H and Lau C N 2012 *Proc. Natl. Acad. Sci. USA* **109** 10802
[24] Min H, Borghi G, Polini M and MacDonald A H 2008 *Phys. Rev. B* **77** 041407(R)
[25] Vafek O and Yang K 2010 *Phys. Rev. B* **81** 041401(R)
[26] Zhang F, Min H, Polini M and MacDonald A H 2010 *Phys. Rev. B* **81** 041402(R)
[27] Nandkishore R and Levitov L 2010 *Phys. Rev. Lett.* **104** 156803
[28] Lemonik Y, Aleiner I L, Toke C and Falko V I 2010 *Phys. Rev. B* **82** 201408(R)
[29] Vafek O 2010 *Phys. Rev. B* **82** 205106
[30] Nandkishore R and Levitov L 2010 *Phys. Rev. B* **82** 115124
[31] Zhang F, Jung J, Fiete G A, Niu Q and MacDonald A H 2011 *Phys. Rev. Lett.* **106** 156801
[32] Jung J, Zhang F and MacDonald A H 2011 *Phys. Rev. B* **83** 115408
[33] Lemonik Y, Aleiner I L and Fal'ko V I 2012 *Phys. Rev. B* **85** 245451
[34] Cvetkovic V, Throckmorton R E and Vafek O 2012 *Phys. Rev. B* **86** 075467
[35] Zhu L, Aji V and Varma C M 2013 *Phys. Rev. B* **87** 035427
[36] Zhang F and MacDonald A H 2012 *Phys. Rev. Lett.* **108** 186804
[37] Scherer M M, Uebelacker S and Honerkamp C 2012 *Phys. Rev. B* **85** 235408
[38] Xu D H, Yuan J, Yao Z J, Zhou Y, Gao J H and Zhang F C 2012 *Phys. Rev. B* **86** 201404
[39] Wang Y, Wang H, Gao J H and Zhang F C 2013 *Phys. Rev. B* **87** 195413
[40] Kresse G and Furthmüller J 1996 *Phys. Rev. B* **54** 11169
[41] Perdew J P, Burke K and Ernzerhof M 1996 *Phys. Rev. Lett.* **77** 3865
[42] Baskaran G 2013 arXiv: 1309.2242 [cond-mat.str-el]
[43] Sorella S and Tosatti E 1992 *Europhys. Lett.* **19** 699
[44] Martelo L M, Dzierzawa M, Siffert L and Baeriswyl D 1997 *Z. Phys. B* **103** 335